Journal of Hydrology 635 (2024) 131164

Contents lists available at ScienceDirect

Journal of Hydrology

journal homepage: www.elsevier.com/locate/jhydrol

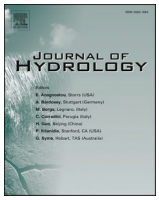

Research papers

New data-based analysis tool for functioning of natural flood management measures reveals multi-site time-variable effectiveness

Martyn T. Roberts [a,b,*], Mark E. Wilkinson [b], Paul D. Hallett [c], Josie Geris [a]

[a] School of Geosciences, University of Aberdeen, Aberdeen, United Kingdom
[b] James Hutton Institute, Aberdeen, United Kingdom
[c] School of Biological Sciences, University of Aberdeen, Aberdeen, United Kingdom

ARTICLE INFO

Keywords:
Temporary storage areas
Runoff attenuation
Nature-based solutions
Natural flood management
Flooding

ABSTRACT

Temporary storage areas (TSAs) are a type of Natural Flood Management measure or nature-based solution that can provide additional storage during flood events by intercepting and attenuating surface runoff. Pressures on land use and an increase in climate change induced storms means there is a need to create additional storage within multifunctional rural landscapes. Implementation of small-scale TSAs is slowly gaining momentum, but practitioners still require further evidence on their functioning during different storm events. Here we present the TSA Drainage Rate Analysis tool (TSA-DRA tool), a novel data-based mechanistic method that only requires rainfall and TSA water level data to describe individual TSA drainage rates. We developed and then used the TSA-DRA tool to perform a multi-site assessment of different TSAs, allowing comparisons of TSA functioning across different types or time-variable factors. TSA design and outlet were found to be the dominant controls on drainage rates when the feature is full. Meanwhile, time-variable differences in functioning were more evident at lower water levels, when soil infiltration was the main TSA outflow. Results from a modelling experiment using observed time-variable TSA drainage rates suggested that these can impact the TSAs flood mitigation effectiveness. Specifically, for a particular event, soil conditions of a TSA in NE Scotland were more effective during spring than winter in attenuating surface runoff. Understanding spatial and temporal differences in TSA drainage rates will help optimise existing and future TSA designs, ensuring small-scale headwater TSAs are successfully integrated within rural catchments to mitigate an increasing exposure to hydrological extremes.

1. Introduction

Changes in land use and an intensification of the hydrological cycle due to climate change are set to exacerbate flood risk globally (Gudmundsson et al., 2021; Merz et al., 2021). Changing rainfall patterns and an increase in rainfall erosivity are also creating additional issues, such as soil erosion and drought (Luetzenburg et al., 2020; Panagos et al., 2022; Pokhrel et al., 2021; Polade et al., 2014). These factors contribute to an increasing complexity of water resource management (Ficklin et al., 2022). Consequently, there is now a need to create additional catchment storage that attenuates surface runoff (Bokhove et al., 2020), which not only mitigates flood risk, but also addresses multiple environmental issues.

Small-scale (<10,000 m^3) headwater temporary storage areas (TSAs) are a type of nature-based solution (NbS) that can create dispersed and new catchment-based storage on land to mitigate flooding and soil erosion (Roberts et al., 2023; Suttles et al., 2021; Wilkinson et al., 2019). They may also be referred to as a Natural Flood Management (NFM) approach or Runoff Attenuation Feature (see Quinn et al., 2022). TSAs can come in a variety of types and volumetric sizes, but are all designed to attenuate runoff by disconnecting quick flow pathways. The design typically ensures that they drain within 1–2 days, maximising their available storage capacity for attenuating subsequent storm events and minimising farmland inundation times and effects on crops (Hewett et al., 2020; Quinn et al., 2022). Small-scale headwater TSAs offer a sustainable solution to catchment management and have been used to mitigate various flooding and erosion challenges around the world (Lucas-borja et al., 2021; Suttles et al., 2021). For example, TSAs have been shown to reduce peak flows by 30 % in the 5.7 km^2 Belford catchment (UK) by providing a total additional ~ 3500 m^3/km^2 of storage (Nicholson et al., 2019). In the Loess Plateau (China), TSAs accounted for a 58 % reduction in soil losses (Zhao et al., 2015) and were

* Corresponding author.
E-mail address: m.roberts.20@abdn.ac.uk (M.T. Roberts).

https://doi.org/10.1016/j.jhydrol.2024.131164
Received 20 December 2023; Received in revised form 15 March 2024; Accepted 18 March 2024
Available online 8 April 2024

effective in trapping coarse silt for soil and water conservation (27–42 % of total sediment content) (Wang et al., 2018). Despite the multiple benefits TSAs can provide, uptake by practitioners remains limited (Brillinger et al., 2021; Raška et al., 2022), with one key evidence gap being how functioning depends on location and varies with time (Ngai et al., 2017; Penning et al., 2023).

A number of empirical studies have explored the functioning of individual TSAs (Lockwood et al., 2022; van Leeuwen et al., 2024). However, there remains limited empirical evidence on how different types of TSAs function, how their functioning is affected by the role of place (e.g., catchment location and soil type) and whether their functioning is time variable. TSA functioning can be described by the relationship between TSA available storage, fill rates (inputs) and drainage rates (outputs). While inputs are mainly a function of the amount and timing of rainfall and catchment characteristics, TSA storage and drainage depend on TSA design and local soil properties (Fennell et al., 2022; Roberts et al., 2023). How TSA storage declines with time after rainfall ultimately determines the TSA available storage for the next rainfall event. Improved understanding of local TSA drainage rates will therefore help address more broadly individual TSA functioning and flood mitigation effectiveness in terms of TSA available storage.

Variations in rainfall, antecedent conditions and soil structure can have implications for both TSA fill and drainage rates (Hankin et al., 2017; Lockwood et al., 2022). The time-variable nature of soil structure, influenced by land management practices such as tillage (O'Connell et al., 2007; Strudley et al., 2008), as well as biological factors, such as vegetation type and cover (Hudek et al., 2022; Lu et al., 2020), suggests that TSA drainage rates may vary over time. Repetitive and prolonged ponding has also been shown to decrease soil infiltration rates (Hallett et al., 2016; Lassabatere et al., 2010; Levine et al., 2021), which would suggest that TSA drainage rates deteriorate with time. Thus, it is important to understand TSA functioning across varying time-variable conditions and determine hydrological thresholds that cause distinct drainage rates.

Currently, there is no systematic approach for characterising the functioning of various TSA types from empirical data (Connelly et al., 2023; Penning et al., 2023). Monitoring of features is steadily increasing, but this is typically limited to rainfall and TSA water level data. There is therefore a need for an approach that relies on such primary data only, while being flexible enough to consider a wide range of TSA designs and site characteristics. Offline ponds (bunds on floodplains) are one of the most extensively studied TSAs (e.g., Ghimire et al., 2014; Lockwood et al., 2022; Nicholson et al., 2019), however existing methods often rely on high-resolution digital elevation models (DEMs) for mass balance analysis or they assume that there are no infiltration losses from the feature. Time-variability is often overlooked as well, but differences in drainage rates may have implications for TSA available storage and their flood mitigation effectiveness. Understanding differences between TSA types and time-variability will help inform both existing and future TSA designs and their management.

The overall aim of this study was to develop and test a systematic approach for characterising TSA functioning which can be applied to a range of TSA types and be used to explore variability in functioning with time. More specifically the objectives were to: (i) develop a data-based mechanistic method for assessing individual TSA drainage rates that can be adapted for all TSA types; use this to (ii) establish whether there are time-variable drainage rates in multi-site TSAs with long-term datasets; (iii) determine if any such time-variable functioning varies across locations or TSA designs; and (iv) explore what the effect is of time-variable drainage rates on TSA functioning for different storm events.

2. Data and methods

2.1. Study sites

The study includes long term (>1 year) data from five headwater TSAs that were different in type and volume, and which were integrated within multifunctional rural landscapes, such as arable, livestock farming and moorland (Fig. 1 and Table 1). All TSAs were in the north-east of the UK, so the prevailing humid temperate climate was comparable. Detailed descriptions of each TSA site were provided by Ghimire et al. (2014) for Tarland, Wilkinson et al. (2010) for Belford and Fennell et al., (2020,2022) for Glenlivet; a brief summary is provided below and in Table 1.

The Tarland bund (Fig. 1 and Table 1) was constructed using soil to reduce the risk of sediment rich overland flow entering a village downstream (Wilkinson et al., 2019). The feature is situated at the field boundary in an existing grass buffer margin. Land use in the contributing area is arable (Table 1), but it has also been used for cattle pasture from late autumn to early spring some years. The arable land becomes inundated when the TSA water level exceeds ~ 10 cm. The Belford offline pond was constructed using hardwood timber panels to create a 'leaky' wall that attenuated runoff and stream spill in the uplands of the Belford Burn (Fig. 1 and Table 1) (Wilkinson et al., 2010) (Table 1). It was also designed to trap sediments and nutrients that were being mobilised from livestock poaching during wet conditions (Nicholson et al., 2012; Wilkinson et al., 2010). The Belford bund was designed to intercept a dominant overland flow pathway and provide a pass for machinery during wet conditions in the lowlands of the Burn (Fig. 1 and Table 1) (Nicholson et al., 2012). At Glenlivet, a sequence of wooden and earth leaky barriers were installed to attenuate runoff in ephemeral streams, thereby improving drought resilience for the distillery by enhancing summer low flows (Fig. 1 and Table 1) (Fennell et al., 2022). Although primarily designed for drought management, they do provide flood mitigation benefits as well, highlighting the multi-benefits TSAs can provide (e.g., Short et al., 2019). The wooden leaky barrier is more of a traditional in-channel feature, whereas the earth leaky barrier is a ~ 0.5 m depression (below ground level) that has no outlet pipe. Soil type within the TSA wetted footprint changes from the peaty topsoil for the wooden leaky barrier, to the exposed freely draining mineral subsoil for the earth leaky barrier. The monitored wooden and earth leaky barriers are located within the same ephemeral stream, with the earth feature being the next TSA downstream from the wooden.

These TSAs were selected for the study as they provide multiple examples of available small-scale headwater TSAs (Roberts et al., 2023), with each TSA either differing in design or catchment setting. This

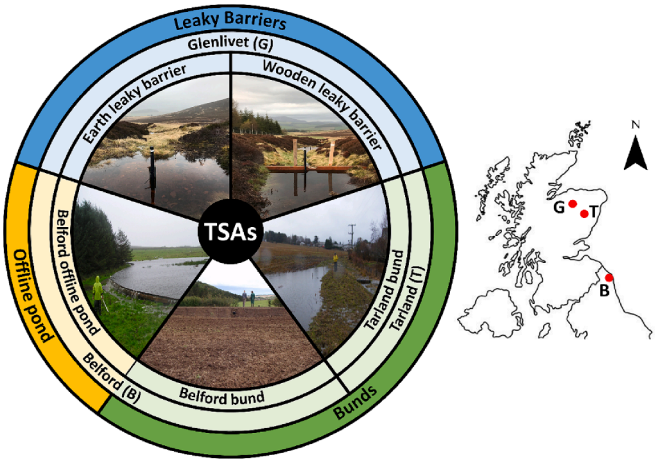

Fig. 1. TSA case studies and location within the NE of the UK for Belford (B), Glenlivet (G) and Tarland (T).

Table 1
TSA dimensions, additional TSA information and catchment characteristics.

	Tarland	**Belford**		**Glenlivet**	
TSA name and type	Tarland bund	Belford bund	Belford offline pond	Wooden leaky barrier	Earth leaky barrier
TSA storage capacity (m^3)	~200	~500	~800	~0.1	~0.2
TSA height (m)	0.5	1	1	0.35	0.5
Outlet design	Pipe	Pipe	Leaky wall	Leaky wall and weir notch	None
Outlet pipe height (m)	0.25	0.5	Multiple gaps	Multiple gaps	NA
Outlet pipe diameter (m)	0.2	0.3	~0.002 gaps	~0.002 gaps	NA
TSA contributing area (km^2)	0.32	0.18	0.5	0.1	0.1
Land use in contributing area	Arable - spring barley / winter wheat	Arable and grass (rotational)	Permanent pasture	Heather	Heather
Sub-surface tile drainage beneath TSA	Yes	Yes	Yes	No	No
Monitoring period	Jul 2015 to Feb 2023	Feb 2010 to Mar 2011	Aug 2008 to Mar 2011	May 2021 to Jul 2023	May 2021 to Jul 2023
Catchment	Tarland Burn (74 km^2), Aberdeenshire (UK)	Belford Burn (5.7 km^2), Northumberland (UK)		Blairfindy (0.9 km^2), Moray (UK)	
Soil	**World Reference Base:** Cambisols **Texture:** Sandy loam to sandy clay **Drainage:** Free	**World Reference Base:** Stagnosols **Texture:** Fine loamy over clayey drift **Drainage:** Poor and seasonal waterlogging		**World Reference Base:** Podzols / Histosols **Texture:** Organic **Drainage:** Free / Poor	
Mean elevation (m.a.s.l.) (m)	~200	~120		~438	
Mean annual rainfall (mm)	~800	~700		~900	

allowed for a broad assessment of TSA functioning and therefore a better understanding of the main factors controlling drainage rates and whether time-variable functioning differed between location or TSA type. A multi-site assessment was chosen to increase the TSA empirical evidence base beyond offline ponds, but also to test the flexibility of the new data-based mechanistic method.

2.2. Data

Local rainfall and TSA water level data were used to assess TSA functioning and effectiveness. At all sites, water level was measured at 15-minute intervals at the lowest point behind the TSA, so it captured the maximum height of each structure. This was collected using pressure transducers (In-Situ Rugged TROLL 100 and van Essen Mini-Diver), which also recorded water temperature. At all experimental sites, rain gauges (0.2 mm tipping buckets) were located near the TSAs (<5 km) and recorded tips were aggregated to provide 15-minute records. Data from nearby weather stations (max. 20 km) were used to provide supplementary meteorological context and included temperature, estimates of potential evapotranspiration (PET) and soil moisture to help describe catchment conditions for each storm event. Storm annual exceedance probability (AEP) estimates were provided by Marsh et al. (2016) for Tarland and by for Wilkinson et al. (2010) and Nicholson et al. (2019) for Belford.

2.3. Data analysis

TSA water level and local rainfall were used to assess TSA functioning and provide an overview of TSA conditions during the monitoring periods. The assessment required water level to identify decreasing segments (recession periods) and the rate at which the feature is draining, while rainfall was used to estimate the time at which there is no surface runoff entering the TSA following the storm event. To provide an overview of TSA functioning during the monitoring period, two water level thresholds were chosen to describe the frequency and inundation times of TSA events. A greater than 10 % water level threshold was chosen to describe how often the features were active and their average inundation time before they returned to near empty levels. A greater than 50 % level threshold was used to show TSA performance at fuller levels, highlighting the potential effect of outlet design (if applicable) on TSA available storage for subsequent events.

2.4. TSA drainage rate analysis tool (TSA-DRA tool)

A new data-based mechanistic method was developed to analyse the drainage rates of TSAs and assess whether time-variable functioning differs across location and TSA design. By focussing on TSA drainage rates, our aim was to address more broadly functionality and how the feature drains following a storm event, leading to a better understanding of factors affecting TSA available storage and their flood mitigation effectiveness. The approach integrates overall functioning over many storms to reduce the variability of individual events and provide a consistent description of drainage. Flexibility was a key consideration during development, ensuring the method's applicability to different types of TSAs and allowing for exploration of variability in TSA functioning between sites and over time.

We therefore developed the TSA Drainage Rate Analysis tool (TSA-DRA tool), which brings together and builds on a set of automated resources. The methods include: (i) extraction of recession periods (Fig. 2a), (ii) creation of a master recession curve (MRC) and (iii) fitting a model to describe TSA drainage (Fig. 2b). The tool has been developed in R programming language (R Core Team, 2021) and is available to be downloaded from an open database (see conclusion for details). The MRC method is a graphical approach that has been previously used for recession analysis of baseflows (Carlotto & Chaffe, 2019; Duncan, 2019; Lamb & Beven, 1997). MRCs overcome the variability of individual recession curves and events by considering several curves over a longer period (Lamb & Beven, 1997; Snyder, 1939; Tallaksen, 1995). MRCs describe the rate of change in discharge over time, offering insights into the dynamics of catchments or streamflow, especially during periods of decreasing water levels (Carlotto & Chaffe, 2019; Lamb & Beven, 1997). Here we use MRCs to determine a consistent description for TSA drainage (Fig. 2b), before exploring time-variable differences at each site (Fig. 2c).

2.4.1. Extracting individual recession curves

The automated extraction of recession curves uses the basic principles of recession analysis (Fig. 2a). Individual recession curves were extracted using five essential criteria with the option to add more, depending on TSA design. The essential criteria for extraction included that there must be periods during which (1) TSA water levels decreased and (2) were at or below the maximum TSA height, (3) there was no additional rainfall, (4) water temperatures were above 0 °C, and (5) the duration of the recession curve exceeded the minimum recession length value.

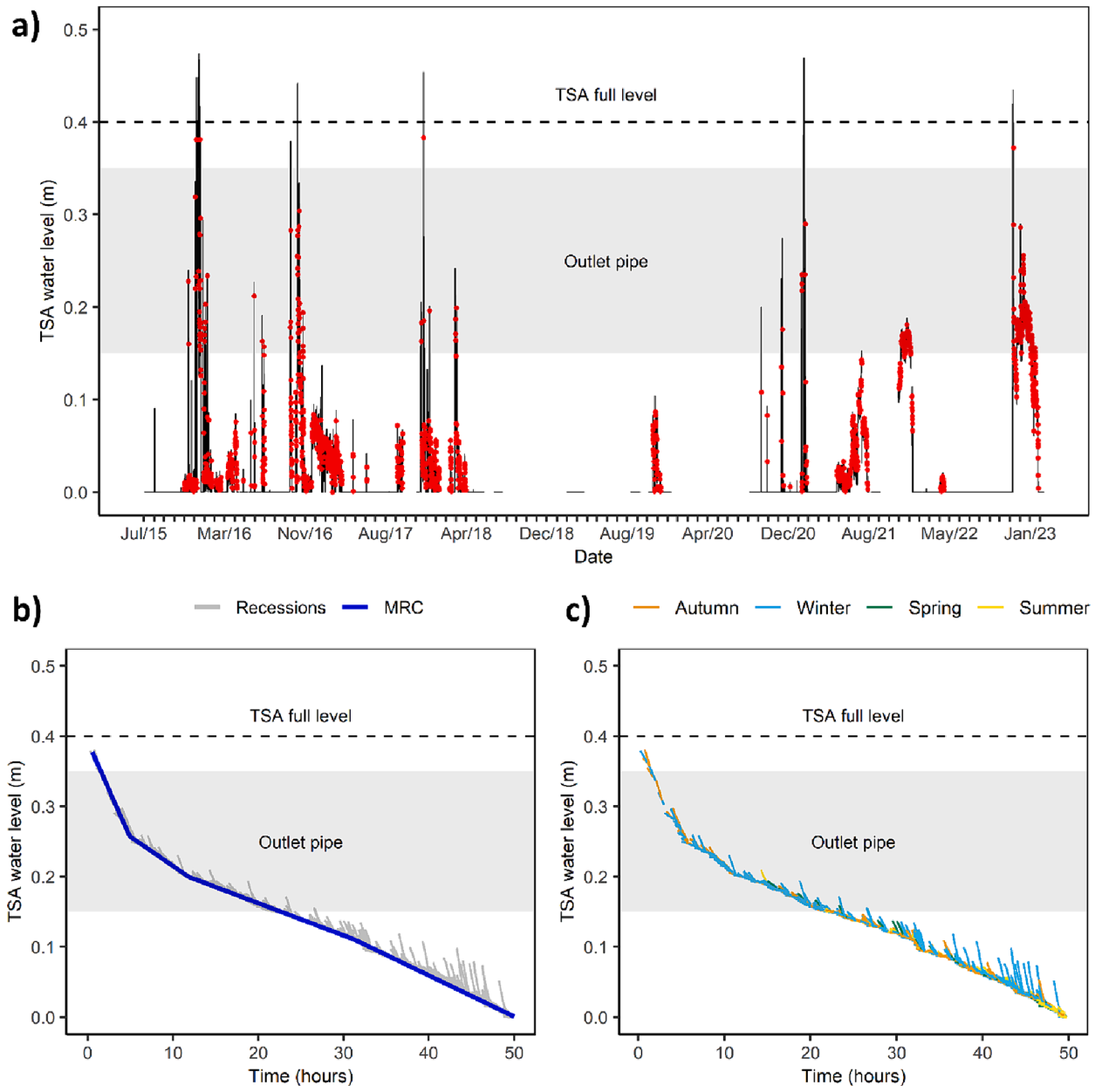

Fig. 2. An example of the TSA drainage rate analysis tool method using the Tarland dataset. a) Extraction of recession curves (red dots) from timeseries that match the recession criteria; b) The creation of the master recession curve (MRC) and the fitting of a segmented linear model to describe TSA drainage; c) Time-variable MRC. (For interpretation of the references to colour in this figure legend, the reader is referred to the web version of this article.)

The first criteria for extracting individual recession curves is a difference in level between consecutive time steps being less than zero ($dL/dt < 0$) (Brutsaert & Nieber, 1977; Carlotto & Chaffe, 2019). Volume can be used instead of level data, however unless high-resolution DEMs are available, there can be uncertainties when quantifying TSA level-volume relationships. The TSA full line was used to identify overflow events and was determined based on field observations during storms. These overflow events were then excluded from drainage rate analysis by only extracting recession curves that were below the TSA full line.

To avoid or minimise additional water entering the TSA during recession analysis, recessions were only extracted following a user defined time value (hours) since the last rainfall. Runoff generation and duration depends on a variety of factors such as, rainfall intensity and duration, soil type, land management, vegetation, antecedent conditions and topography (Castillo et al., 2003; O'Connell et al., 2007; Panagos et al., 2022). Therefore, the time value that relates to the length of the dry period after rainfall cessation should be site specific and user informed. Following a series of laboratory experiments, Ran et al. (2012) estimated that runoff can last up to ~ 20 minutes following the event. The dry period after rainfall cessation should also be informed by the TSA type and desired drainage rate analysis. For example, larger volumed TSAs such as bunds and offline ponds (Table 1) normally have an outlet pipe to maximise available storage and thus, are only temporarily full during larger storm events (Wilkinson et al., 2019). To assess TSA drainage from full to empty would therefore require a smaller dry period after rainfall cessation. A moving window sum that is the equivalent length of the user defined time value since last rainfall (e.g., 2 h) was applied to the rainfall timeseries. Recessions were then extracted when cumulative precipitation was less than the maximum precipitation negligibility value, which by default was set to 0.2 as it represents one tip of the rain gauge.

To avoid errors with frozen water behind the TSA, the user can set a

TSA water temperature value, whereby recessions are extracted when the water temperature is greater than the specified value (here 0 °C). Finally, the extracted recessions were filtered so the length of each recession period is equal to or greater than the minimum recession duration value (e.g., >= 1 h). The essential criteria for the extraction of individual recessions are summarised in Equation (1):

$$Recessions = dL/dt < 0 \;\&\; L < TSA\,full\,level \;\&\; cum.P \leq max.P\_neg \;\&\; T > water_T^{TSA} \;\&\; R_{dur} > minR_{dur} \quad (1)$$

where L is level (m), dL/dt is difference in level between time steps (m), $cum.P$ is cumulative precipitation (mm), $max.P\_neg$ is maximum precipitation negligibility (mm), T is temperature threshold for frozen water (°C), $water_T^{TSA}$ is the TSA water temperature value (°C), R_{dur} is the recession duration (hours), and $minR_{dur}$ is the minimum recession duration.

User defined values were built into the recession extraction method so it could be applied to multiple TSA designs and locations. Vogel and Kroll (1992) suggested that for recession analysis a moving average should be applied to suppress noise, so a 5-point moving average was applied to 15-minute record water level data. For the Tarland bund and Belford TSAs, the dry period after rainfall cessation was set at 2 h to limit surface runoff input and the minimum recession duration was set at 1 h to ensure there was enough data at fuller levels. The dry period after rainfall cessation was adjusted to 8 h for the Glenlivet leaky barriers to try and limit the volume of surface and subsurface runoff input. The minimum recession duration was also increased to 2 h to provide a better representation of drainage, which was achievable due to more TSA events (data) for these features. An additional recession criterion was used for the Belford offline pond (Fig. 1 and Table 1), whereby recessions were extracted when the stream stage was less than the stream spill height. If desired, the user could look solely at soil infiltration by only extracting recessions when the TSA water level is less than the outlet height. The extraction criteria should result in enough recession curves to create the MRC, ensuring there is overlap between individual curves across the full TSA level range (Carlotto & Chaffe, 2019; Duncan, 2019; Lamb & Beven, 1997; Snyder, 1939).

2.4.2. Automated master recession curve (MRC)

Several approaches for MRC determination have been used previously, including the matching strip method (Snyder, 1939) and correlation method (Langbein, 1938). The TSA-DRA tool uses the matching strip method for MRC determination (Fig. 2b), as it is the most commonly used approach in other studies (e.g., Carlotto & Chaffe, 2019), and has been found to be approximately one order of magnitude more accurate than the correlation method (Nathan & McMahon, 1990). The correlation method involves plotting the level at one time point (L_t) against level one time interval later (L_{t+dt}) for the selected recession periods, and a curve then fitted to the data.

The matching strip method involves sorting recession curves by minimum values (high to low). Recession curves are then moved so the positional index of the minimum value for each recession coincides with the position of the corresponding value in the immediate lower curve. Finally, a curve is fitted to the minimum value of each time interval. However, the matching strip method traditionally only utilises the lower end of each recession. Therefore, time-variable differences in recession curves may not be fully captured. An additional step was added to the beginning of the matching strip method, where each recession was split so they were equal to the recession duration value. This means that more segments of each recession curve are used to create the MRC and they are overlapped based on the slope gradient at that depth rather than at the lower end.

2.4.3. Fitting a model to the master recession curve (MRC)

For fitting a model to the MRC, a segmented linear model approach was chosen to simplify the analysis and ensure that the method was transferable between TSA types that may have different drainage patterns (Fig. 2b). Segmented linear models were fitted to the MRC points using the 'segmented' package in R programming (Muggeo, 2008). It is an iterative procedure (Muggeo, 2003) that requires initial breakpoint estimates. The algorithm is made less sensitive to initial breakpoint estimates by implementing bootstrap restarting (Wood, 2001). The segmented regression model is estimated and provides relevant approximate standard errors of all model parameters, including breakpoints. To ensure the method is consistent, the automated 'strucchange' package (Zeileis et al., 2002) was used to estimate initial breakpoint values. The 'breakpoints' function uses the algorithm described in Bai and Perron (2003) for simultaneous estimation of multiple breakpoints. It detects structural breaks in the timeseries and then optimises the performance of the regression model by selecting the optimal number of breakpoints and their corresponding x-axis values.

2.4.4. Time-variability

The above method was repeated with additional extraction criteria to explore seasonal and annual variability (Fig. 2c). Seasonality was used to assess the effects of temporal changes in soil structure due to both natural (e.g. weather) and land management (e.g. tillage) factors as well as the impact of antecedent conditions (Lu et al., 2020; Quinn et al., 2022; Strudley et al., 2008). Analysis of TSA drainage rates between years was done to determine if the features degraded following prolonged and repetitive ponding (Lassabatere et al., 2010; Levine et al., 2021).

2.5. Modelling the impact of time-variable drainage rates on TSA available storage

To explore the impact of any time-variable funtioning of TSAs on their effectiveness to capture and store runoff for flood management, we used a simple water balance modelling approach to evaluate the effects of variable drainage rates on TSA available storage. Specifically, we applied winter and spring TSA drainage rates to TSA functioning of the Tarland bund. This TSA had the most comprehensive dataset, including a large storm event that caused widespread flooding in December 2015 - January 2016 across NE Scotland. The peak flow for the River Dee (2100 km^2) during this event was estimated to have a 0.5 % AEP (Marsh et al., 2016). Tarland bund level (m) was converted into volume (m^3) using a depth-volume relationship that was estimated from a 1 m Lidar DEM.

For any given TSA, we can assume that the TSA inputs equal the TSA outputs and a change in storage, following Equation (2):

$$inputs(surface\,runoff + subsurface\,flow + direct\,precipitation)_{(t)} = dS_{(t)} - outputs(soil\,infiltration + outlet\,pipe + overflow + PET)_{(t-1)} \quad (2)$$

For which inputs (m^3/15 min), outputs (m^3/15 min), and dS(t) (m^3) is the observed volume for each time interval.

To estimate the outputs of the TSA water balance model at any given volume, conditional statements and empirical based equations were used to define drainage via soil infiltration, outlet pipe and overflow. Soil infiltration rates were derived from the general MRC for the Tarland bund, which uses the entire dataset to create a general description of drainage. The drainage rate of the general MRC for when water level was less than the height of the outlet pipe was used to represent soil infiltration (Equation (3)):

$$\textbf{\textit{If TSA water level}} < \textbf{\textit{outlet pipe height}}$$
$$Soil\,infiltration = Tarland\,bund\,general\,MRC\,(< outlet\,pipe\,height) \quad (3)$$

Due to insufficient above outlet pipe data for some time-variable MRCs, Torricelli's formula was used to estimate outlet pipe discharge by

assuming hydrostatic flow through a small orifice (Equation (4)):

$$\textit{If TSA water level} > \textit{outlet pipe height}$$
$$\textit{Outlet pipe} = C_d A\sqrt{2gH} \quad (4)$$

where H is TSA water level (m), A is cross-sectional area of the outlet pipe (m^2), g is gravitational acceleration (9.8 m/s^2) and C_d is coefficient discharge, which was set at 0.65 and typically ranges between 0.61 and 0.75 depending on the orifice type (Hicks & Slaton, 2014). This approach standardised outlet pipe discharge between time-variable scenarios and it was used to represent TSA drainage when water level was above the outlet height. Overflow was calculated by subtracting the maximum TSA storage (200 m^3) from the TSA volume. Finally, PET was calculated in mm using the Penman–Monteith method from local weather station data and converted to m^3 by using the wetted area of the TSA.

The sum of the TSA outputs for each time interval and difference in volume (dS) from observed data was then used to estimate the TSA inputs for each time interval, according to Equation (2). To explore the impact of time-variable drainage rates on TSA effectiveness (Equation (5)), TSA outputs were recalculated for given TSA volumes, but using spring and winter MRCs to describe soil infiltration instead of the general MRC.

$$dS_{(t)} = TSA\ inputs_{(t)} - TSA\ outputs_{(t-1)} \quad (5)$$

3. Results

3.1. TSA events and wider hydroclimatological conditions

We found high variability in the inundation characteristics of the different TSA types included in the study (Table 2, Fig. 3). This can be associated with differences in TSA design, although local TSA storage dynamics and function are also dependent on rainfall and catchment properties. For example, the earth leaky barrier (no pipe outlet) had similar inundation times above thresholds greater than 10 % and 50 % full (90 and 82.5 days/year, respectively), whereas there were significant differences in these relative inundation times for TSAs with a pipe or other outlet (Table 2). TSAs with smaller volumes, such as the Glenlivet leaky barriers, regularly reached fuller levels which may also be due to their positioning within an ephemeral stream (online TSA) (Table 2 and Fig. 3).

For TSAs with larger volumes, such as the Tarland bund and Belford offline pond, pipe outlets only tended to become active during significant storm events, mainly in autumn and winter months (Fig. 3). Throughout the timeseries, soil infiltration was therefore the dominant TSA outflow. Large storm events were observed across the TSA case studies that caused the features to reach full levels. For example, a 2 % AEP storm event occurred at the Belford offline pond in September 2008, following significantly higher monthly rainfall totals than the long-term average during June, July and August (Fig. 3b). During this event, 96 mm of rain fell over a 36-hour period. Both Belford TSAs reached fuller levels during the March 2010 event, with 59 mm and 77 mm of rainfall recorded for the previous two days (Fig. 3b). AEP was estimated at 20 % and 8 % for the daily rainfall totals. However, TSA level fullness was ~ 75 % for the offline pond compared to ~ 45 % for the bund (Fig. 3b). The Tarland bund frequently overflowed in January 2016, following a prolonged period of intense rainfall, where daily totals of precipitation reached highs of 44 mm (Fig. 3a) and peak flow for the River Dee (2100 km^2) had an estimated 0.5 % AEP. In November 2022, the Tarland bund and both Glenlivet TSAs were active following excessive wet conditions. Maximum daily rainfall totals were 65 mm at Tarland and 31 mm at Glenlivet (Fig. 3).

3.2. Time-variable TSA drainage rates

The general drainage behaviour of the TSAs was found to be comparable for similarly structured TSAs (i.e., larger volumes and TSA outlets), such as the Tarland bund, Belford bund and offline pond (Fig. 4a). These TSAs exhibited an exponential decay MRC shape, requiring 50 to 70 h for complete emptying. Meanwhile, the smaller-volumed wooden leaky barrier had more of a linear MRC shape, taking ~ 40 h to empty (Fig. 4a). The earth leaky barrier, characterised by below-ground level storage and no outlet, showed an increasing negative MRC slope, typically taking ~ 60 h to empty (Fig. 4a). It is important to note that using volume instead of level may yield different MRC shapes, but the time to empty will remain the same.

Despite differences between TSA case studies (volume and location), the outlet design played an important role in maintaining available storage when levels exceed ~ 50 % fullness (Fig. 4a and Table 2). TSAs with an outlet tend to have an inundation time of ~ 10 h for these events (Fig. 4a and Table 2). This is characterised by steeper drainage at fuller levels, which is equal to ~ 28 mm/hr at the Tarland bund, ~37 mm/hr at the Belford offline pond and ~ 23 mm/hr at the wooden leaky barrier (Fig. 4a). The drainage rate decreased with level for TSAs with an outlet, as the main outflow switched to soil infiltration (Fig. 4a and Table 2). All TSAs have further drainage via the soil that will operate at the same time as outlet flow, albeit at much slower rates. This is evident in the earth leaky barrier (no outlet), where the MRC shape remains fuller for longer (Fig. 4). However, as the TSA level decreases, the drainage rate increases (~38 mm/hr) (Fig. 4).

Seasonal time variability was most evident at the Tarland bund, Belford offline pond and earth leaky barrier, while the Belford bund and wooden leaky barrier showed comparatively less variability (Fig. 4b). Meanwhile, inter-annual time-variability was most clearly observed at the Tarland bund and earth leaky barrier, and less so at the Belford TSAs and Glenlivet wooden leaky barrier (Fig. 4c). Where observed, time-variable differences in drainage rates were most noticeable at lower TSA levels (<50 %) when the dominant outflow is via soil infiltration (Fig. 4). Seasonal MRCs indicated a general trend whereby spring drainage was the quickest and winter the slowest (Fig. 4b). For example, at Tarland the drainage rate below the outlet pipe reached highs of ~ 21 mm/hr in spring, compared to ~ 5.5 mm/hr for other seasons. It is worth noting that TSAs which create additional above ground level storage (i.e., Tarland bund, Belford TSAs and Glenlivet wooden leaky barrier) had

Table 2
Summary of TSA water level data and inundation times.

Site	TSA type	TSA full level (m)	>10 % TSA level fullness				>50 % TSA level fullness			
			n	Mean n per year	Mean inundation (days)	Mean inundation (days/year | (%year))	n	Mean n per year	Mean inundation (days)	Mean inundation (days/year | (%year))
Tarland	Bund	0.4	661	85	0.4	34 | (9.5 %)	34	4	0.4	2 | (0.5 %)
Belford	Bund	1	40	37	0.25	9.5 | (2.5 %)	0	0	0	0
	Offline pond	1	153	58	0.5	29 | (8 %)	14	5	0.4	2 | (0.5 %)
Glenlivet	Wooden leaky barrier	0.35	90	42	1.5	58 | (16 %)	96	45	0.5	27 | (7.5 %)
	Earth leaky barrier	0.5	45	21	4.5	90 | (25 %)	45	21	4	82.5 | (22.5 %)

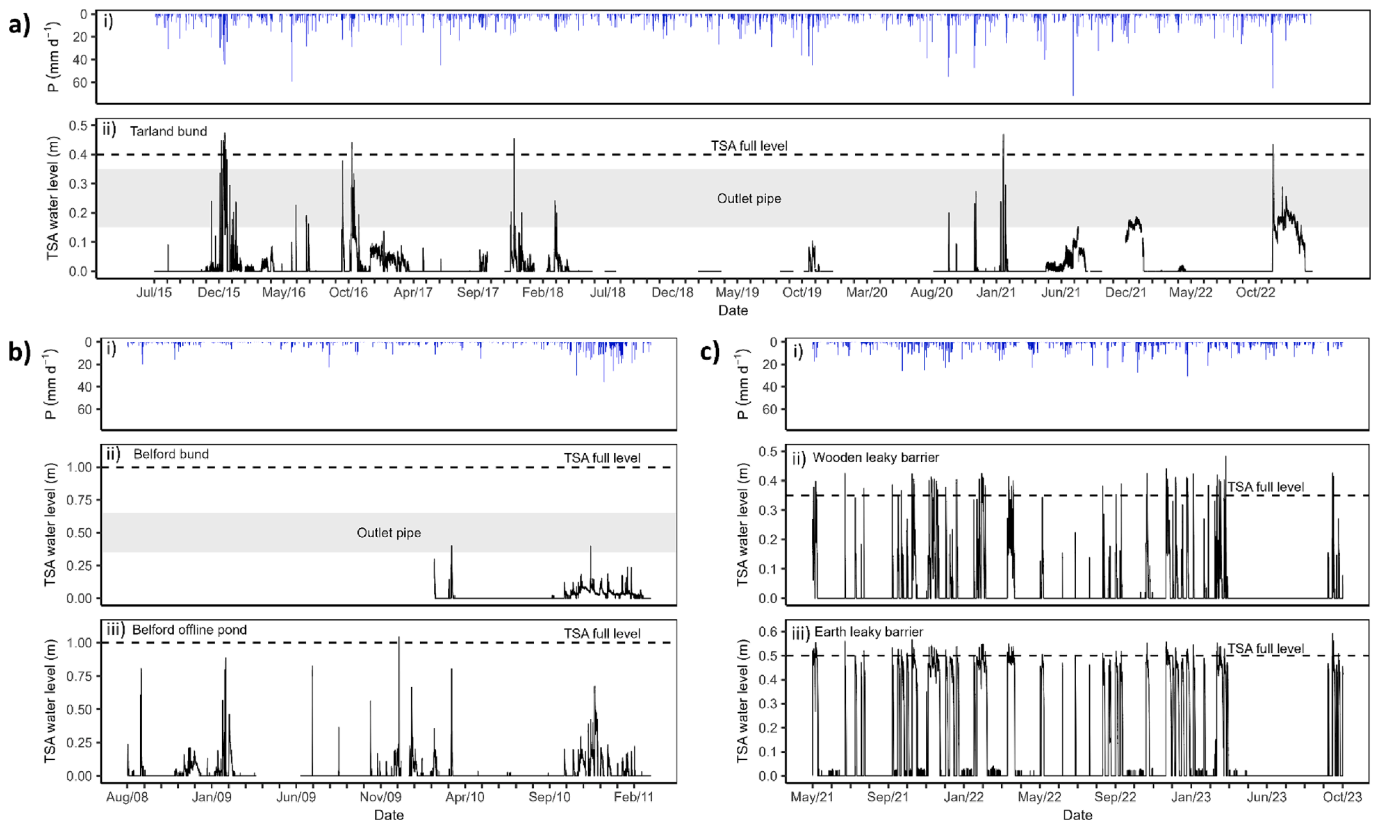

Fig. 3. TSA timeseries data. a) Tarland, b) Belford, c) Glenlivet, i) = precipitation (P), ii - iii) = TSA water level.

fewer observations at fuller levels (>50 %) during spring and summer, due to drier antecedent conditions (Fig. 3). The Tarland bund displayed the most inter-annual variability, with the greatest drainage rates occurring in 2015 (installation year) and 2020 (Fig. 4c), although this site also had the longest record. The Glenlivet earth leaky barrier appeared to take longer to drain in 2022, which coincided with settling and increased sedimentation following installation (2021) (Fig. 4c).

3.3. The impact of time-variable drainage rates on TSA available storage

Observed data from a multiday storm event (0.5 % AEP) between December 2015 and January 2016 at the Tarland bund were used for the TSA model to explore the potential effect of time-variable TSA drainage rates (Fig. 5). Prolonged rainfall resulted in a series of overflow events occurring, with the maximum TSA volume of water behind the feature reaching ~ 240 m^3 (Fig. 5). Precipitation (total of 270 mm in 21 days) reached a peak intensity of 6 mm/hr (Fig. 5a). Fig. 5b shows the estimated TSA inputs and outputs when deriving soil infiltration rates from the general MRC (Fig. 4a). Soil infiltration rates were then changed to explore the effect of winter versus spring scenarios (Fig. 4b) on the TSA available storage.

Figure 6 demonstrates how time-variable differences in soil infiltration can impact TSA flood mitigation effectiveness during large storm events. The drainage rates as observed in spring provide relatively more available storage for longer, compared to the drainage rates as observed in winter (Fig. 6a). This means that for the same event (from Fig. 5), there would be less overtopping (Fig. 6b) and outflow from the outlet pipe (Fig. 6c), corresponding to more soil infiltration (Fig. 6d) for spring TSA drainage rates as opposed to winter TSA drainage rates. Figure 6a suggests that there was no difference between time-variable scenarios when the feature was full (low TSA available storage), which can be related to the outlet pipe being the dominant outlfow (max. ~ 40 m^3/15 min) (Fig. 6c) and being of a much higher magnitude than soil infiltration (Fig. 6d). Figure 6b reveals that when using spring drainage conditions, the frequency and magnitude of overflow was less compared to using winter drainage conditions, suggesting that soil inflitration rates and antecedent conditions affect TSA flood mitigation effectiveness.

4. Discussion

4.1. TSA-DRA tool and the role of design on TSA functioning

The TSA-DRA tool provides a new systematic approach for characterising TSA functioning, specifically drainage, across a wide range of TSA types and sizes. As part of its flexibility, it provides a fully empirical, data-based mechanistic method, which has relatively few data demands given it relies only on precipitation and TSA level data. The TSA-DRA tool guarantees transferability among TSA types (Fig. 1) and holds relevance for other NbS features, such as sustainable drainage systems (SuDs). It serves as a valuable resource for enhancing understanding of individual TSA functionality and effectiveness, contributing to the NbS and NFM empirical evidence base (Connelly et al., 2023; Penning et al., 2023). It hereby adds to other NFM studies that have used data-based methods to quantify the hydrological impact of interventions at the catchment scale (Mindham et al., 2023; van Leeuwen et al., 2024). The TSA-DRA tool also possesses the capability to estimate soil infiltration rates, a parameter that has not always been considered or quantified in prior TSA studies. This estimation provides an important function for TSA modelling (Fig. 6). The adaptability of the TSA-DRA tool allows for the investigation of time-variable functionality and effectiveness, thereby addressing a constraint previously recognised in the adoption of TSAs by practitioners (Ngai et al., 2017; Raška et al., 2022). Nevertheless, conducting time-variable analysis requires longer datasets with an adequate number of TSA filling events, which may not always be available. One other challenge lies in characterising all TSA inputs,

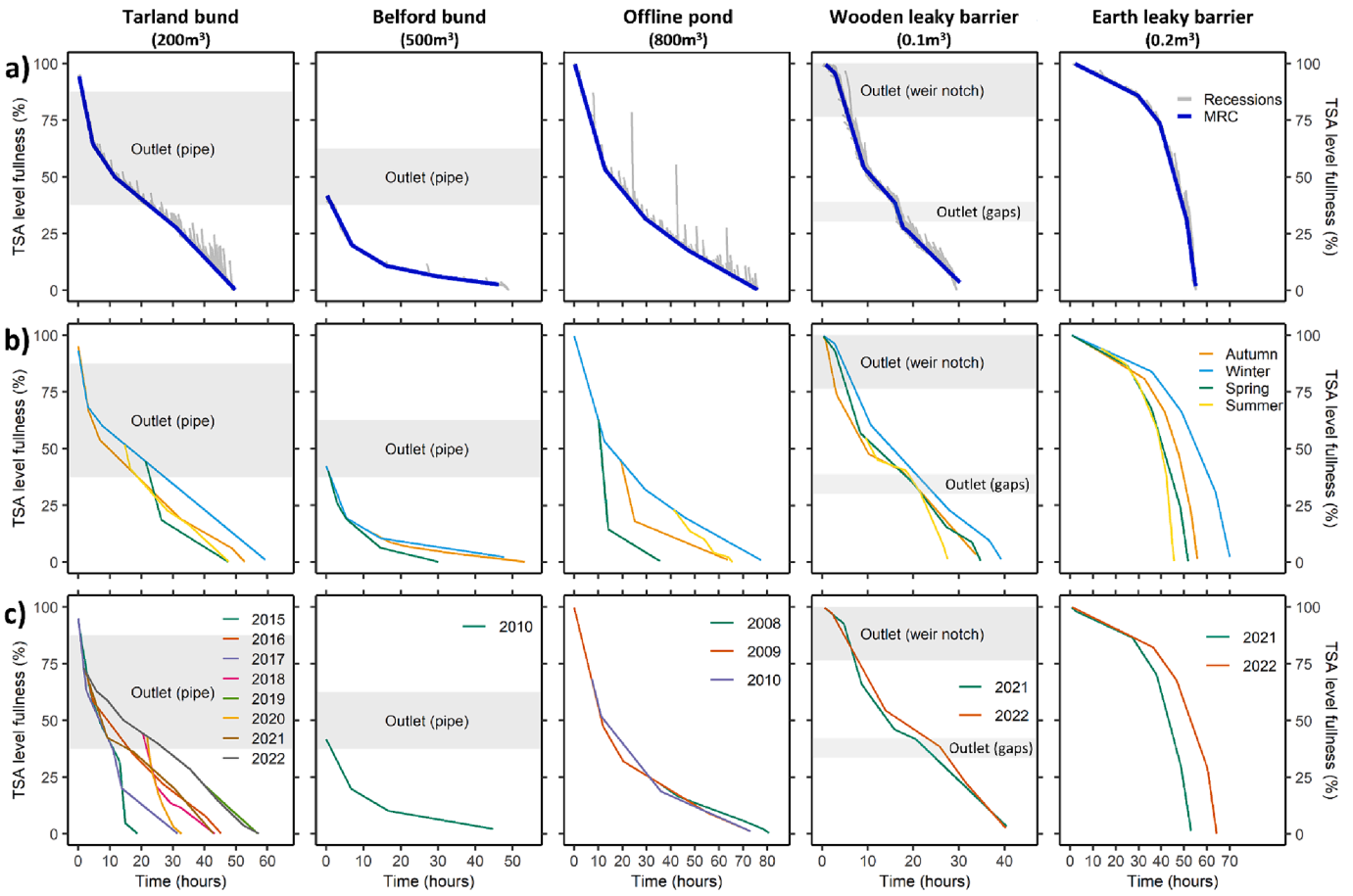

Fig. 4. TSA time-variable master recession curves (MRCs). a) general MRCs, b) seasonal MRCs, c) annual MRCs.

specifically additional surface and subsurface flow, especially when assessing drainage rates at fuller TSA levels.

Application of the TSA-DRA tool to data from five different TSAs revealed how TSA functioning can vary specifically based on design (Table 2 and Fig. 4). Ultimately, the TSA design is typically specific to its local context (Ngai et al., 2017). Nevertheless, despite variations in total storage between local TSAs, a general finding was that the design of the outlet determined the dominant outflow when levels exceeded 50 % fullness and thus an important factor for maintaining available storage (Fig. 6). Metcalfe et al. (2018) suggested that NFM storage features should have retention times of the order of 10 h to maximise their impact on large flow peaks and subsequent storm events. The earth leaky barrier and Belford offline pond (Fig. 4), revealed longer retention times, potentially diminishing their effectiveness for a sequence of events. Outlets should provide an appropriate discharge that maximises available storage during multiday storm events, thereby reducing the risk of overflow (Fig. 6) (Lucas-borja et al., 2021; Metcalfe et al., 2018). When TSAs are full, their flood mitigation effectiveness diminishes as they only provide a small reduction in velocity due to drag and longer flow pathways (Nicholson et al., 2019). However, the slower drainage rates observed here at lower TSA levels (Fig. 4), are typically linked to longer retention times. When converted to volume, these slower drainage rates at lower levels may have a negligible impact on the available storage for subsequent events. In addition, the earth leaky barrier at Glenlivet was primarily designed to maximise groundwater recharge and has no outlet, which accounts for its longer retention times. It is possible that the Belford bund outlet was too large due to no greater than 50 % fullness occurrences (Table 2). When TSAs are positioned on productive land, the outlet design should ensure that there is minimal impact on farm productivity by reducing inundation times at fuller levels (e.g. Tarland bund) (Hewett et al., 2020). The earth leaky barrier illustrates the impact of having no outlet and storage below ground level, resulting in extended inundation periods (Table 2 and Fig. 4). A delayed response to subsurface flow, coupled with the TSA-DRA tool's limitation of not excluding all TSA inputs at fuller levels, may result in a longer inundation time for the earth leaky barrier. The drainage rate of the earth leaky barrier increases as the level decreases, most likely due to less subsurface input and a higher soil infiltration rate associated with the mineral subsoil that was exposed during installation (Fig. 4). Understanding the soils and geology within the TSA footprint is therefore important when considering TSA design, especially when there is no outlet (Fennell et al., 2022; Levine et al., 2021; Reaney, 2022).

Beyond the outlet pipe, subsurface tile drainage can be used to maintain infiltration rates within the TSA footprint, with varying levels of success dependent on the design, soil type and condition. However, there could be a risk of exporting nutrient-rich waters into faster subsurface pathways. Therefore, these drains should be managed at strategic locations (e.g., end of drain wetlands) where appropriate (Barber & Quinn, 2012). The Tarland and Belford bunds share similar designs, yet they exhibit variations in drainage rates beneath the outlet pipes (Fig. 4a), most likely due to disparities in soil properties and field drainage systems (Table 1). Subsurface tile drainage can help maintain local functioning by increasing soil water storage capacity (Marshall et al., 2009). However, they can deteriorate due to physical damage, infilling by soil and plant roots or soil structural degradation causing less effective water transport (Hallett et al., 2016). Soil structural degradation can be exacerbated when drainage is impeded within wetter soils, with surface sealing (Assouline & Mualem, 2001) and greater slumping occurring (Augeard et al., 2008). Field drainage systems can vary in design and spacing, but site specific knowledge is often sparse due to

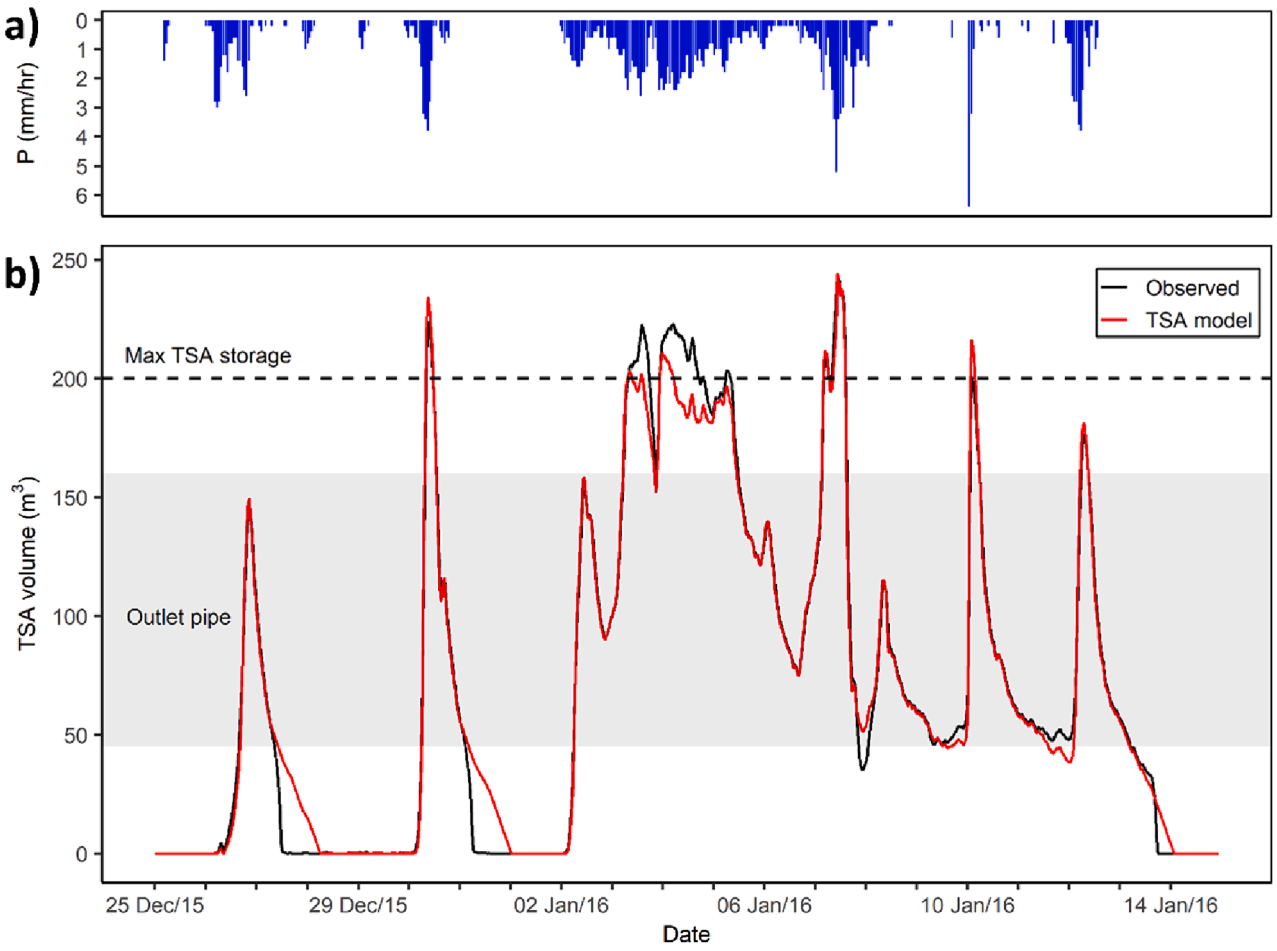

Fig. 5. Winter 2015/16 storm period at the Tarland bund. a) hourly precipitation (P), b) estimated volume of water behind TSA.

limited historical records (installed 50–100 years ago) (Hallett et al., 2016). The differences in MRC shape between bunded TSAs may also result from the use of level instead of volume data. If accurate DEMs were available for each site to convert level to volume, they would have most likely displayed an exponential decay fit. This is due to the combined impacts of hydraulic head on drainage rate and of surface topography on water storage.

4.2. TSA functioning through time

Time-variable functioning of TSAs was most prominent at the Tarland bund, Belford offline pond, and earth leaky barrier, particularly at lower TSA levels, where soil infiltration was the dominant outflow (Fig. 4). Soil properties can undergo alterations in short timeframes, influenced by factors such as major weather events or tillage (Levine et al., 2021; Strudley et al., 2008), as well as over extended periods through agricultural and biological activity (Hudek et al., 2022; Lu et al., 2020). Seasonal MRCs identified that TSAs generally drained slowest in winter and quickest in spring (Fig. 4b). Initial soil water content in surface layers is an important control on runoff and infiltration, particularly in low intensity storms (Castillo et al., 2003). Therefore, seasonal MRC differences may be attributed to wetter antecedent conditions in winter and drier conditions in spring. In peatland systems (Glenlivet), soils are susceptible to shrinkage during dry conditions (Seidel et al., 2023), resulting in less recession events in the summer due to rapid drainage (Fig. 3 and Fig. 4b). However, soil time-variability has minimal significance for the wooden leaky barrier, due to the engineering design and associated undercutting or seepage around the small-scale feature (Fig. 4).

The degradation and regeneration of soil structure are key factors that could explain time-variable disparities in TSA functioning observed in Fig. 4. Frequent inundation during the wetter autumn and winter months could cause coalescence of the soil structure and the reduction of macropores (Ghezzehei & Or, 2000; Levine et al., 2021). Erosional deposits have also been shown to reduce infiltration capacities (Lassabatere et al., 2010; Levine et al., 2021). Wetter soils within the TSA footprint at the Tarland and Belford TSAs may also be vulnerable to compaction by livestock, resulting in the formation of an anisotropic soil pore system (Hamza & Anderson, 2005). Meanwhile, the growth of plant roots and restoration of soil structure might explain enhanced drainage rates observed in spring (Fig. 4b) (Hudek et al., 2022; Lu et al., 2020). At Tarland, a significant area of the TSA footprint covers arable soils. Consequently, tillage serves as a means to reset the topsoil structure following inundation, enabling landowners to reincorporate sediment-rich soils back into the field (Fig. 4c) (Robotham et al., 2023). Levine et al. (2021) previously suggested that infiltration rates decline with time, which is evident for the earth leaky barrier due to increased sedimentation and erosional deposits not being removed. It is worth noting that annual MRC variability was influenced by the dominant recession events for that year, meaning they may reflect certain antecedent conditions, land use or vegetation.

TSA flood mitigation effectiveness was found to be influenced by time-variable drainage rates (Fig. 6), highlighting the significance of antecedent conditions and temporal changes in soil structure on TSA performance (Lockwood et al., 2022; Quinn et al., 2022). Understanding the dynamic nature of drainage rates not only improves knowledge of how TSAs function during different storms (Ngai et al., 2017; Raška et al., 2022), but also offers the potential for design optimisation. For

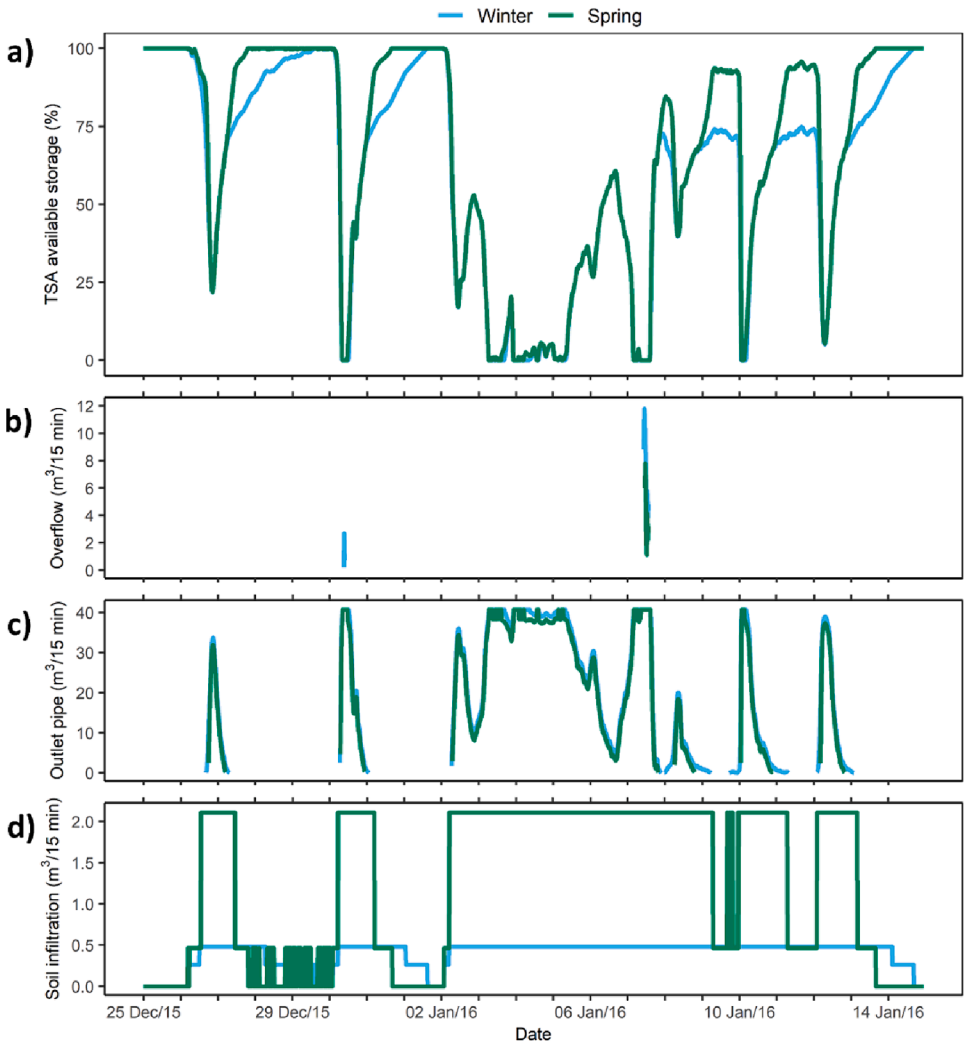

Fig. 6. Impact of time-variable drainage rates on the Tarland bund's available storage during a large storm event.

example, adjustable outlets could be used to manage time-variable functioning, allowing for faster or slower drainage rates as required, as demonstrated at Holnicote (National Trust, 2015).

4.3. Optimising TSA designs and management strategies

NFM design tools could be employed before implementation to optimise outlet design and retention times (e.g., Follett et al., 2023). Alternatively, hydrological modelling could inform outlet design (Hankin et al., 2017), or adjustments could be made post-installation based on empirical data analysis (Nicholson et al., 2012), including TSA-DRA. Enhancing soil infiltration rates within the TSA footprint could also improve functioning, thereby affecting TSA available storage for both small and large storm events (Fig. 6). Soil infiltration serves as the primary outflow for larger-volume TSAs in the more common small to medium storm events, with outlets only becoming active during exceptionally wet conditions (Table 2 and Fig. 3). For example, soil infiltration accounts for approximately 65 % drainage of the cumulative volume of water stored behind the Tarland bund across the ~ 8-year monitoring period. Stutter et al. (2020) describe the concept of '3D buffers' and how soft-engineering and vegetation management within field boundary margins or TSAs, could be used to optimise functionality and address other issues. For example, vegetation within the TSA footprint could be used to improve infiltration rates (Hudek et al., 2022; Lu et al., 2020), whilst tackling diffuse pollution through nutrient uptake and increasing biodiversity (Stutter et al., 2020; Zak et al., 2019). Maintaining year-round vegetation cover within the TSA footprint has the potential to boost soil organic carbon content and aggregate stability, consequently mitigating the risk of soil structural degradation (Hamza & Anderson, 2005). Roots of cover crops can also be used to bio-engineer agricultural soils. Hudek et al. (2022) found that species which possess greater root length and surface area, such as oat, rye, and buckwheat, can significantly increase topsoil porosity in compacted soil at 30 cm depth. However, in the deeper compacted subsoil at 50 cm depth, only mustard and radish improved soil porosity. Periodic tillage at Tarland was found to alleviate the effects of frequent and prolonged inundation (Fig. 4c). This highlights the potential for integrating TSAs within agricultural lands, offering improved TSA functioning through tillage and advantages to landowners in terms of soil and nutrient retention (Robotham et al., 2023; Strudley et al., 2008). However, the development of a plough pan impedes vertical infiltration and enhances interflows (Bertolino et al., 2010), and once formed, they can persist for decades and be challenging to alleviate (Jones et al., 2003).

It is important that TSAs remain multifunctional in their design, but trade-offs and tensions can arise between the primary and additional benefits. For example, below ground level storage associated with the earth leaky barrier resulted in longer inundation times (Table 2 and Fig. 4), which is not desirable when the inundated land is for example, used for agriculture, but would be better suited for biodiversity, soil erosion and water conservation (Fennell et al., 2022; Robotham et al.,

2023). Additional benefits are often missed and can be difficult to quantify when assessing the value of NbS (Connelly et al., 2023; Short et al., 2019). Glenlivet provides an example of how a sequence of TSAs could be strategically employed to address multiple catchment issues by adapting the primary function of each feature.

5. Conclusions

This study presents a new data-based and systematic approach for characterising TSA functioning, with the results from a multi-site analysis contributing to the NbS and NFM empirical evidence base. The novel TSA-DRA tool revealed various factors that influence TSA drainage rates. We found that TSA functioning changed through time due to temporal changes in soil structure and antecedent conditions. This was most evident at lower water levels, when soil infiltration was the dominant outflow. TSA outlet and design were found to be crucial for regulating available storage when the feature is full. The TSA-DRA tool provided important soil infiltration estimations, which were utilised to model the impact of time-variability on TSA effectiveness. The TSA modelling results emphasise the importance of time-variable factors, highlighting less overflow for the spring soil infiltration scenario compared to winter during a large storm event.

Soil infiltration emerged as the dominant TSA outflow during small to medium storm events. Future research should focus on monitoring temporal changes in soil structure and their impacts on TSA functioning. The TSA modelling exercise revealed the potential of well-structured soils to improve TSA flood mitigation effectiveness. This could inform the development of management strategies aimed at optimising TSA performance and addressing time-variable differences. While this study enhances understanding of individual TSAs, future research should assess the effectiveness of TSAs at the catchment scale. This would entail exploring optimal methods for distributing additional storage within headwater catchments and considering the influence of location, scale, and time on TSA flood mitigation effectiveness.

Enhanced insights into TSA functionality and time-variable nuances are invaluable for shaping future design and management strategies. This knowledge is crucial when implementing small-scale headwater TSAs, particularly with the mounting complexity of water resource management and hydrological extremes. The TSA-DRA tool offers invaluable insights into the functioning of various TSA types, highlighting the significance of time-variable drainage rates on TSA flood mitigation effectiveness.

The TSA-DRA tool is an open source and is available from: https://github.com/martynr27/TSA-DRA-tool.git.

CRediT authorship contribution statement

Martyn T. Roberts: Writing – review & editing, Writing – original draft, Visualization, Validation, Software, Project administration, Methodology, Investigation, Formal analysis, Data curation, Conceptualization. **Mark E. Wilkinson:** Writing – review & editing, Validation, Supervision, Resources, Funding acquisition, Data curation. **Paul D. Hallett:** Writing – review & editing, Validation, Supervision, Funding acquisition. **Josie Geris:** Validation, Supervision, Methodology, Funding acquisition, Formal analysis, Conceptualization, Writing – review & editing.

Declaration of competing interest

The authors declare that they have no known competing financial interests or personal relationships that could have appeared to influence the work reported in this paper.

Data availability

Data will be made available on request and the TSA-DRA tool is available to be downloaded from https://github.com/martynr27/TSA-DRA-tool.git

Acknowledgements

Thanks to the Scottish Government's Hydro Nation Scholars Programme for funding MR to do this research. MW received funding from the Scottish Government's Rural and Environment Sciences Analytical Services Division (JHI- D2-2) which enabled his contributions and supported the collection of wider hydrometric datasets in the Tarland catchment. JG and MW acknowledge funding from NERC (NE/P010334/1) and Chivas Brothers (Glenlivet). In relation to Tarland, we wish to acknowledge the MacRobert Estate, local landowners and Carol Taylor and Helen Watson for their assistance with fieldwork. For Glenlivet, we wish to acknowledge Dr Ronald Daalmans, staff at the Glenlivet distillery and Dr Jessica Fennell and Dr Eva Loerke for their assistance with fieldwork. We would like to thank Dr Paul Quinn in relation to Belford. We are grateful to Prof Keith Beven who provided constructive comments that helped to improve the quality of the manuscript.

References

Assouline, S., Mualem, Y., 2001. Soil seal formation and its effect on infiltration: Uniform versus nonuniform seal approximation. Water Resources Research 37 (2), 297–305. https://doi.org/10.1029/2000WR900275.

Augeard, B., Bresson, L.M., Assouline, S., Kao, C., Vauclin, M., 2008. Dynamics of soil surface bulk density: Role of water table elevation and rainfall duration. Soil Science Society of America Journal 72 (2), 412–423. https://doi.org/10.2136/sssaj2006.0429.

Bai, J., Perron, P., 2003. Computation and analysis of multiple structural change models. Journal of Applied Econometrics 18 (1), 1–22. https://doi.org/10.1002/jae.659.

Barber, N.J., Quinn, P.F., 2012. Mitigating diffuse water pollution from agriculture using soft-engineered runoff attenuation features. Area 44 (4), 454–462. https://doi.org/10.1111/j.1475-4762.2012.01118.x.

Bertolino, A.V.F.A., Fernandes, N.F., Miranda, J.P.L., Souza, A.P., Lopes, M.R.S., Palmieri, F., 2010. Effects of plough pan development on surface hydrology and on soil physical properties in Southeastern Brazilian plateau. Journal of Hydrology 393 (1–2), 94–104. https://doi.org/10.1016/j.jhydrol.2010.07.038.

Bokhove, O., Kelmanson, M.A., Kent, T., Piton, G., Tacnet, J.M., 2020. A cost-effectiveness protocol for flood-mitigation plans based on Leeds' Boxing Day 2015 Floods. Water 12 (3), 652. https://doi.org/10.3390/w12030652.

Brillinger, M., Henze, J., Albert, C., Schwarze, R., 2021. Integrating nature-based solutions in flood risk management plans: A matter of individual beliefs? Science of the Total Environment 795, 148896. https://doi.org/10.1016/j.scitotenv.2021.148896.

Brutsaert, W., Nieber, J.L., 1977. Regionalized drought flow hydrographs from a mature glaciated plateau. Water Resources Research 13 (3), 637–643.

Carlotto, T., Chaffe, P.L.B., 2019. Master Recession Curve Parameterization Tool (MRCPtool): Different approaches to recession curve analysis. Computers and Geosciences 132, 1–8. https://doi.org/10.1016/j.cageo.2019.06.016.

Castillo, V.M., Gómez-Plaza, A., Martínez-Mena, M., 2003. The role of antecedent soil water content in the runoff response of semiarid catchments: A simulation approach. Journal of Hydrology 284 (1–4), 114–130. https://doi.org/10.1016/S0022-1694(03)00264-6.

Connelly, A., Snow, A., Carter, J., Wendler, J., Lauwerijssen, R., Glentworth, J., Barker, A., Handley, J., Haughton, G., Rothwell, J., 2023. What approaches exist to evaluate the effectiveness of UK-relevant natural flood management measures? A Systematic Map. *Environmental Evidence* 12 (1), 1–22. https://doi.org/10.1186/s13750-023-00297-z.

Duncan, H.P., 2019. Baseflow separation – A practical approach. Journal of Hydrology 575, 308–313. https://doi.org/10.1016/j.jhydrol.2019.05.040.

Fennell, J., Geris, J., Wilkinson, M.E., Daalmans, R., Soulsby, C., 2020. Lessons from the 2018 drought for management of local water supplies in upland areas: A tracer-based assessment. Hydrological Processes 34 (22), 4190–4210. https://doi.org/10.1002/hyp.13867.

Fennell, J., Soulsby, C., Wilkinson, M.E., Daalmans, R., Geris, J., 2022. Assessing the role of location and scale of Nature Based Solutions for the enhancement of low flows. International Journal of River Basin Management 1–16. https://doi.org/10.1080/15715124.2022.2092490.

Ficklin, D.L., Null, S.E., Abatzoglou, J.T., Novick, K.A., Myers, D.T., 2022. Hydrological intensification will increase the complexity of water resource management. *Earth's*. Future 10 (3), e2021E–F002487. https://doi.org/10.1029/2021EF002487.

Follett, E., Beven, K., Hankin, B., Mindham, D., & Chappell, N. (2023). The importance of retention times in Natural Flood Management interventions. *Proc. IAHS*, *100*, 1–5. Accessed on [8th March 2024] via University of Liverpool Repository: https://livrepository.liverpool.ac.uk/id/eprint/3177004.

Ghezzehei, T.A., Or, D., 2000. Dynamics of soil aggregate coalescence governed by capillary and rheological processes. Water Resources Research 36 (2), 367–379. https://doi.org/10.1029/1999WR900316.

Ghimire, S., Wilkinson, M.E., Donaldson-Selby, G., 2014. Application Of 1D And 2D Numerical Models For Assessing And Visualizing Effectiveness Of Natural Flood Management (NFM). In: Measures. *11th International Conference on Hydroinformatics*, p. 9.

Gudmundsson, L., Boulange, J., Do, H.X., Gosling, S.N., Grillakis, M.G., Koutroulis, A.G., Leonard, M., Liu, J., Schmied, H.M., Papadimitriou, L., Pokhrel, Y., Seneviratne, S.I., Satoh, Y., Thiery, W., Westra, S., Zhang, X., Zhao, F., 2021. Globally observed trends in mean and extreme river flow attributed to climate change. Science 371 (6534), 1159–1162. https://doi.org/10.1126/science.aba3996.

Hallett, P. D., Hall, R., Lilly, A., Baggaley, N. J., Crooks, B., Ball, B., Raffan, A., Braun, H., Russell, T., Aitkenhead, M., Riach, D., Rowan, J. S., & Long, A. (2016). *Effect of Soil Structure and Field Drainage on Water Quality and Flood Risk*. https://www.crew.ac.uk/sites/www.crew.ac.uk/files/publication/CRW2014_03_Soil_Structure_Drainage_Flood_Risk_Main_Report.pdf.

Hamza, M.A., Anderson, W.K., 2005. Soil compaction in cropping systems: A review of the nature, causes and possible solutions. Soil and Tillage Research 82 (2), 121–145. https://doi.org/10.1016/j.still.2004.08.009.

Hankin, B., Metcalfe, P., Johnson, D., Chappell, N. A., Page, T., Craigen, I., Lamb, R., & Beven, K. J. (2017). Strategies for testing the impact of natural flood risk management measures. In T. V. Hromadka & P. Rao (Eds.), *Flood Risk Management* (pp. 1–39). IntechOpen. Doi: 10.5772/intechopen.68677.

Hewett, C.J.M., Wilkinson, M.E., Jonczyk, J., Quinn, P.F., 2020. Catchment systems engineering: An holistic approach to catchment management. Wiley Interdisciplinary Reviews: Water 7 (3), e1417.

Hicks, A., Slaton, W., 2014. Determining the coefficient of discharge for a draining container. The Physics Teacher 52 (1), 43–47. https://doi.org/10.1119/1.4849155.

Hudek, C., Putinica, C., Otten, W., De Baets, S., 2022. Functional root trait-based classification of cover crops to improve soil physical properties. European Journal of Soil Science 73 (1), e13147.

Jones, R.J.A., Spoor, G., Thomasson, A.J., 2003. Vulnerability of subsoils in Europe to compaction: A preliminary analysis. Soil and Tillage Research 73 (1–2), 131–143. https://doi.org/10.1016/S0167-1987(03)00106-5.

Lamb, R., & Beven, K. J. (1997). Using interactive recession curve analisys to specify a general catchment storage model. *Hydrological and Earth System Sciences*, *1*(1), 101–113. Hydrology and Earth System Science.

Langbein, W.B., 1938. Some channel-storage studies and their application to the determination of infiltration. Eos, Transactions American Geophysical Union 19 (1), 435–447. https://doi.org/10.1029/TR019i001p00435.

Lassabatere, L., Angulo-Jaramillo, R., Goutaland, D., Letellier, L., Gaudet, J.P., Winiarski, T., Delolme, C., 2010. Effect of the settlement of sediments on water infiltration in two urban infiltration basins. Geoderma 156 (3–4), 316–325. https://doi.org/10.1016/j.geoderma.2010.02.031.

Levine, B., Horne, D., Burkitt, L., Tanner, C., Sukias, J., Condron, L., Paterson, J.H., 2021. The ability of detainment bunds to decrease surface runoff leaving pastoral catchments: Investigating a novel approach to agricultural stormwater management. Agricultural Water Management 243, 106423. https://doi.org/10.1016/j.agwat.2020.106423.

Lockwood, T., Freer, J., Michaelides, K., Brazier, R.E., Coxon, G., 2022. Assessing the efficacy of offline water storage ponds for natural flood management. Hydrological Processes 36 (6), e14618.

Lu, J., Zhang, Q., Werner, A.D., Li, Y., Jiang, S., Tan, Z., 2020. Root-induced changes of soil hydraulic properties – A review. Journal of Hydrology 589, 125203. https://doi.org/10.1016/j.jhydrol.2020.125203.

Lucas-borja, M.E., Piton, G., Yu, Y., Castillo, C., Antonio, D., 2021. Check dams worldwide : Objectives, functions, effectiveness and undesired effects. Catena 204, 105390. https://doi.org/10.1016/j.catena.2021.105390.

Luetzenburg, G., Bittner, M.J., Calsamiglia, A., Renschler, C.S., Estrany, J., Poeppl, R., 2020. Climate and land use change effects on soil erosion in two small agricultural catchment systems Fugnitz – Austria, Can Revull – Spain. Science of the Total Environment 704, 135389. https://doi.org/10.1016/j.scitotenv.2019.135389.

Marsh, T., Kirby, C., Muchan, K., Barker, L., Henderson, E., & Hannaford, J. (2016). *The winter floods of 2015/2016 in the UK - a review*. http://nora.nerc.ac.uk/515303/1/N515303CR.pdf.

Marshall, M.R., Francis, O.J., Frogbrook, Z.L., Jackson, B.M., McIntyre, N.R., Reynolds, B., Solloway, I., Wheater, H.S., Chell, J., 2009. The impact of upland land management on flooding: results from an improved pasture hillslope. Hydrological Processes 23 (3), 464–475. https://doi.org/10.1002/hyp.7157.

Merz, B., Blöschl, G., Vorogushyn, S.D., Aerts, F., Jeroen, C.J.H., Bates, P., Bertola, M., Kemter, M., Kreibich, H., Lall, U., Macdonald, E., 2021. Causes, impacts and patterns of disastrous river floods. Nature Reviews Earth & Environment 2 (9), 592–609. https://doi.org/10.1038/s43017-021-00195-3.

Metcalfe, P., Beven, K.J., Hankin, B., Lamb, R., 2018. A new method, with application, for analysis of the impacts on flood risk of widely distributed enhanced hillslope storage. Hydrology and Earth System Sciences 22 (4), 2589–2605. https://doi.org/10.5194/hess-22-2589-2018.

Mindham, D., Beven, K., Chappell, N., 2023. Rainfall–streamflow response times for diverse upland UK micro-basins: quantifying hydrographs to identify the nonlinearity of storm response. Hydrology Research 54 (2), 233–244. https://doi.org/10.2166/nh.2023.115.

Muggeo, V.M.R., 2003. Estimating regression models with unknown break-points. Statistics in Medicine 22 (19), 3055–3071. https://doi.org/10.1002/sim.1545.

Muggeo, V.M.R., 2008. segmented: an R Package to Fit Regression Models with Broken-Line Relationships. R News 8 (1), 20–25. https://cran.r-project.org/doc/Rnews/.

Nathan, R.J., McMahon, T.A., 1990. Evaluation of automated techniques for base flow and recession analyses. Water Resources Research 26 (7), 1465–1473. https://doi.org/10.1029/WR026i007p01465.

Ngai, R., Wilkinson, M. E., Nisbet, T. R., Harvey, R., Addy, S., Burgess-gamble, L., Rose, S., Maslen, S., Nicholson, A. R., Page, T., Jonczyk, J., & Quinn, P. F. (2017). *Working with Natural Processes - Evidence Directory Appendix 2: Literature review*. https://assets.publishing.service.gov.uk/media/6036c5c2d3bf7f0ab0702a25/Working_with_natural_processes_evidence_directory_appendix_2_literature_review.pdf.

Nicholson, A.R., Wilkinson, M.E., O'Donnell, G.M., Quinn, P.F., 2012. Runoff attenuation features: a sustainable flood mitigation strategy in the Belford catchment. UK. *Area* 44 (4), 463–469. https://doi.org/10.1111/j.1475-4762.2012.01099.x.

Nicholson, A.R., O'Donnell, G.M., Wilkinson, M.E., Quinn, P.F., 2019. The potential of runoff attenuation features as a Natural Flood Management approach. Journal of Flood Risk Management 13, e12565.

O'Connell, E., Ewen, J., O'Donnell, G.M., Quinn, P.F., 2007. Is there a link between agricultural land-use management and flooding? Hydrology and Earth System Sciences 11 (1), 96–107. https://doi.org/10.5194/hess-11-96-2007.

Panagos, P., Borrelli, P., Matthews, F., Liakos, L., Bezak, N., Diodato, N., Ballabio, C., 2022. Global rainfall erosivity projections for 2050 and 2070. Journal of Hydrology 610, 127865. https://doi.org/10.1016/j.jhydrol.2022.127865.

Penning, E., Peñailillo Burgos, R., Mens, M., Dahm, R., de Bruijn, K., 2023. Nature-based solutions for floods AND droughts AND biodiversity: Do we have sufficient proof of their functioning? Cambridge Prisms: Water 1, e11.

Pokhrel, Y., Felfelani, F., Satoh, Y., Boulange, J., Burek, P., Gädeke, A., Gerten, D., Gosling, S.N., Grillakis, M.G., Gudmundsson, L., Hanasaki, N., Kim, H., Koutroulis, A. G., Liu, J., Papadimitriou, L., Schewe, J., Müller Schmied, H., Stacke, T., Telteu, C.E., Wada, Y., 2021. Global terrestrial water storage and drought severity under climate change. Nature Climate Change 11 (3), 226–233. https://doi.org/10.1038/s41558-020-00972-w.

Polade, S.D., Pierce, D.W., Cayan, D.R., Gershunov, A., Dettinger, M.D., 2014. The key role of dry days in changing regional climate and precipitation regimes. Scientific Reports 4 (1), 1–8. https://doi.org/10.1038/srep04364.

Quinn, P.F., Hewett, C.J.M., Wilkinson, M.E., Adams, R., 2022. The Role of Runoff Attenuation Features (RAFs) in Natural Flood Management. Water 14 (23), 3807. https://doi.org/10.3390/w14233807.

R Core Team. (2021). *R: A Language and Environment for Statistical Computing*. https://www.r-project.org/.

Ran, Q., Su, D., Li, P., He, Z., 2012. Experimental study of the impact of rainfall characteristics on runoff generation and soil erosion. Journal of Hydrology 424–425, 99–111. https://doi.org/10.1016/j.jhydrol.2011.12.035.

Raška, P., Bezak, N., Ferreira, C.S.S., Kalantari, Z., Banasik, K., Bertola, M., Bourke, M., Cerdà, A., Davids, P., Madruga de Brito, M., Evans, R., Finger, D.C., Halbac-Cotoara-Zamfir, R., Housh, M., Hysa, A., Jakubínský, J., Solomun, M.K., Kaufmann, M., Keesstra, S.D., Hartmann, T., 2022. Identifying barriers for nature-based solutions in flood risk management: An interdisciplinary overview using expert community approach. Journal of Environmental Management 310, 114725. https://doi.org/10.1016/j.jenvman.2022.114725.

Reaney, S.M., 2022. Spatial targeting of nature-based solutions for flood risk management within river catchments. Journal of Flood Risk Management 15 (3), e12803.

Roberts, M.T., Geris, J., Hallett, P.D., Wilkinson, M.E., 2023. Mitigating floods and attenuating surface runoff with temporary storage areas in headwaters. Wires Water 10 (3), e1634.

Robotham, J., Old, G., Rameshwaran, P., Sear, D., Trill, E., Bishop, J., Gasca-Tucker, D., Old, J., McKnight, D., 2023. Nature-based solutions enhance sediment and nutrient storage in an agricultural lowland catchment. Earth Surface Processes and Landforms 48 (2), 243–258. https://doi.org/10.1002/esp.5483.

Seidel, R., Dettmann, U., Tiemeyer, B., 2023. Reviewing and analyzing shrinkage of peat and other organic soils in relation to selected soil properties. Vadose Zone Journal 22 (5), e20264.

Short, C., Clarke, L., Carnelli, F., Uttley, C., Smith, B., 2019. Capturing the multiple benefits associated with nature-based solutions: Lessons from a natural flood management project in the Cotswolds. UK. *Land Degradation and Development* 30 (3), 241–252. https://doi.org/10.1002/ldr.3205.

Snyder, F.F., 1939. A conception of runoff-phenomena. Eos, Transactions American Geophysical Union 20 (4), 725–738. https://doi.org/10.1029/TR020i004p00725.

Strudley, M.W., Green, T.R., Ascough, J.C., 2008. Tillage effects on soil hydraulic properties in space and time: State of the science. Soil and Tillage Research 99 (1), 4–48. https://doi.org/10.1016/j.still.2008.01.007.

Stutter, M., Wilkinson, M. E., & Nisbet, T. R. (2020). *3D buffer strips: Designed to deliver more for the environment*. https://assets.publishing.service.gov.uk/government/uploads/system/uploads/attachment_data/file/1041662/3D_buffer_strips__designed_to_deliver_more_for_the_environment_-_report.pdf.

Suttles, K.M., Eagle, A.J., McLellan, E.L., 2021. Upstream solutions to downstream problems: Investing in rural natural infrastructure for water quality improvement and flood risk mitigation. Water 13 (24), 3579. https://doi.org/10.3390/w13243579.

Tallaksen, L., 1995. A review of baseflow recession analysis. Journal of Hydrology 165 (1–4), 349–370. https://doi.org/10.1016/0022-1694(95)92779-d.

National Trust. (2015). *From source to sea - Natural Flood Management - The Holnicote Experience*. https://nt.global.ssl.fastly.net/holnicote-estate/documents/from-source-to-sea—natural-flood-management.pdf.

van Leeuwen, Z.R., Klaar, M.J., Smith, M.W., Brown, L.E., 2024. Quantifying the natural flood management potential of leaky dams in upland catchments, Part I: A data-based modelling approach. Journal of Hydrology 628 (September 2023), 130448. https://doi.org/10.1016/j.jhydrol.2023.130448.

Vogel, R.M., Kroll, C.N., 1992. Regional geohydrologic-geomorphic relationships for the estimation of low-flow statistics. Water Resources Research 28 (9), 2451–2458.

Wang, W., Fang, N., Shi, Z., Lu, X., 2018. Prevalent sediment source shift after revegetation in the Loess Plateau of China: Implications from sediment fingerprinting in a small catchment. Land Degradation and Development 29 (11), 3963–3973. https://doi.org/10.1002/ldr.3144.

Wilkinson, M.E., Quinn, P.F., Welton, P., 2010. Runoff management during the September 2008 floods in the Belford catchment. Northumberland. *Journal of Flood Risk Management* 3 (4), 285–295. https://doi.org/10.1111/j.1753-318X.2010.01078.x.

Wilkinson, M.E., Addy, S., Quinn, P.F., Stutter, M., 2019. Natural flood management: small-scale progress and larger-scale challenges. Scottish Geographical Journal 135 (1–2), 23–32. https://doi.org/10.1080/14702541.2019.1610571.

Wood, S.N., 2001. Minimizing model fitting objectives that contain spurious local minima by bootstrap restarting. Biometrics 57 (1), 240–244. https://doi.org/10.1111/j.0006-341X.2001.00240.x.

Zak, D., Stutter, M., Jensen, H.S., Egemose, S., Carstensen, M.V., Audet, J., Strand, J.A., Feuerbach, P., Hoffmann, C.C., Christen, B., Hille, S., Knudsen, M., Stockan, J., Watson, H., Heckrath, G., Kronvang, B., 2019. An assessment of the multifunctionality of integrated buffer zones in Northwestern Europe. Journal of Environmental Quality 48 (2), 362–375. https://doi.org/10.2134/jeq2018.05.0216.

Zeileis, A., Leisch, F., Hornik, K., Kleiber, C., 2002. strucchange: An R Package for Testing for Structural Change in Linear Regression Models. Journal of Statistical Software 7 (2), 1–38. https://doi.org/10.18637/jss.v007.i02.

Zhao, G., Klik, A., Mu, X., Wang, F., Gao, P., Sun, W., 2015. Sediment yield estimation in a small watershed on the northern loess plateau, china. Geomorphology 241, 343–352. https://doi.org/10.1016/j.geomorph.2015.04.020.